Flutter Condition Estimation for 3-D Cantilever Plate Using Fully Coupled Fluid – Structure Interaction

Dr.Hayder Sabah Abd Al-Amir
Institute of Technology, Engineering of Technical Education / Baghdad
Email:hyder286@yahoo.com
Dr. Mauwafak Ali Tawfik
Mechanical Engineering Department, University of Technology / Baghdad
Dr.Mohammed Idris Abu-Tabikh
Mechanical Engineering Department, University of Technology / Baghdad

Received on: 4/5/2014 & Accepted on :6/11/2014

ABSTRACT:

The aeroelastic responses and the flutter condition of 3-D flexible cantilever plate were estimated by developed fully coupled fluid-structure interaction(FSI) approach. The plate model (structure model) based on assumed mode method was then combined with unsteady panel-discrete vortex method (aerodynamic model) to build relatively simple aeroelastic model. The validity of the present method had tested through comparisons with the related published work of plates flutter prediction and with wind tunnel measurements.

Time domain simulation is used to examine the dynamic aeroelastic instabilities of the system. The flutter occurrence is verified when the responses diverge. To estimate the flutter frequency, Fast Fourier Transformation (FFT) technique is used to convert the generalized coordinates responses from time domain to frequency domain. The flutter speed and flutter frequency is found for many Aluminum cantilever plates which are different in aspect ratio. The speed and frequency of the flutter are within average absolute error of about 13% and 16 % for theoretical analysis and practically respectively.

Keywords: Aeroelasticity , Fluid-structure interaction, Plate flutter

تخمين الرفرفة لصفيحة كابولية ثلاثية الابعاد باستخدام تداخل التام المائع –الهيكل

الخلاصة

تم تخمين الاستجابة الديناميكية الهوائية و حالة الرفرفة لصفيحة كابولية ثلاثية الأبعاد بواسطة تطوير اسلوب تداخل التام للمائع –الهيكل. تم ربط نموذج الصفيحة (نموذج الهيكل) والمبني على أساس طريقة فرض النسق مع طريقة الأشرطة والدوامات المنفصلة غير المستقرة (النموذج الايروديناميي) لبناء طريقة موثوقة وبسيطة نسبيا للتداخل بين المائع والهيكل. فعالية هذه الطريقة تم اختبارها من خلال مقارنتها مع الاعمال المنشورة التي تتنبئ بحالة الرفرفة للصفائح ومن خلال قياسات العملية لنفق الريح.

استخدام المحاكاة المجال الزمني لفحص عدم الاستقرار للديناميكية الهوائية للنظام. تم التحقق من حدوث رفرفة عندما تبداء الاستجابات بالتباعد . لتخمين تردد الرفرفة ، استخدمت تقنية تحويلة فورير السريعة لتحويل الاستجابات الزمنية للاحداثيات العامة الى مجال التردد. تم التنبئ بسرعة الرفرفة وتردد رفرفة لعدد من صفائح الألومنيوم الكابولية و التي تختلف في النسبة الباعية والنتائج اظهرت توافق جيد مع الأعمال المنشورة.

https://doi.org/10.30684/etj.32.12A.14
2412-0758/University of Technology-Iraq, Baghdad, Iraq
This is an open access article under the CC BY 4.0 license http://creativecommons.org/licenses/by/4.0

Nomenclacure

A_n=adjacent area of the node (m^2)
a=semi span of the wing (m)
b=chord of the wing (m)
C_P= pressure coefficient
E=modules of elasticity (Pa)
h= plate thickness (m)
FSI=fluid-structure interaction
F_n= concentrated force (N)
h_{root}=plate thickness at root (m)
h_{tip}= plate thickness at tip (m)
k_{ij}=stiffness element (N/m)
L=length of panel (m)
m= mass per unit area (kg/m^2)
m_{ij}=mass element (kg)
$\vec{n}$ =normal unit vector
Q_i=generalized force (N)
q_i= generalized coordinate (m)
u=velocity component in x-direction (m/sec)
u_s=deformation of mid surface in x-direction (m)
v_s= deformation of mid surface in y-direction (m)
v=velocity component in z-direction (m/sec)
V_∞ =air velocity (m/sec)
V_{FR}=induced velocity due to unsteady motion of wing (m/sec)
w=plate displacement in z-direction (m)
α =angle of attack (rad)
α_{eff} = effective angle of attack (rad)
Γ =circulation (m^2/sec)
γ=vorticity strength (m/sec)
γ_{xy} =shear strain
ΔP = pressure difference (Pa)
Δt = time step (sec)
δ=node displacement (m)
ε_x =normal strain in x-direction
ε_y = normal strain in y-direction
υ =Poisson's ratio
ϕ = velocity potential (m^2/sec)
ψ_i =coordinate function

INTRODUCTION:

The estimation of flutter condition of vibrating cantilever plate depends mainly on the model used, system parameters and initial conditions. Closed form model (e.g., Thedorsen model [1]), numerical model and experimental works are approaches which were used in this field. In the closed form model, the estimation

of flutter speed is based on identification of the critical condition where one of the roots has zero real part.

In the numerical model (like the present model) the flutter speed may be estimated from the behavior of time displacements responses of the generalized coordinates. In this method the aerodynamic forces are calculated by solving the basic fluid dynamic equations numerically with direct effective interaction with the structure solver.

Nejad [2] has found the flutter speed and flutter frequency for different aspect ratios of cantilever plate. It was assumed that the flow about the plate was incompressible, in viscid and irrigational and a 3-D unsteady vortex lattice method was used in the aerodynamic model. The fluid-structure interaction analysis was solved by using time domain eigenmode analysis. Eloy [3] developed a theoretical model that enables the modeling of the flutter of a rectangular cantilever plate in axial flow. The plate deflection was assumed two-dimensions and immersed in a three dimensional potential in viscid flow .Gakerkin method was used to derive the equations of motion for the plate .

The in viscid fluid forces on the plate had been calculated in Fourier space assuming a finite plate span. The stability of the plate as function of mass ratio, plate aspect ratio and flow speed was studied. Chen et al. [4 and 5] had developed a fully coupled methodology between fluid and structure for 2-D flow induced vibrations. In their method, the Roe scheme was extended to the moving grid system. The unsteady solutions march in time by using a dual-time stepping implicit unfiltered Gauss-Seidel iteration. The unsteady Navier–Stokes equations and the structural equations were fully coupled implicitly via successive iteration within each physical time step.

The difficulties in published theoretical 3-D aero elastic analysis may be summarized as follows:

1-The ways of exchanging the information between the aerodynamic model and structure model during the solution is the surface fitting which not give high accuracy.

2-For viscous flow, the solution requires the mesh generation, and re-generation of mesh at each time step.

This leads to: huge data resulting from solving the FSI problem need high capacity for the computer, and long running time.

In the present approach, the difficult in surface fitting is avoided by converting the aerodynamic pressures to concentrated forces by multiplying the value of pressure at each node by adjacent area of the node. Then these forces will be introduced to the structure equation as discrete forces. This reduces the mathematical processes, resulting data and save time comparing with the methods which used in published works.

In present FSI approach, a hybrid panel-discrete vortex unsteady method combined with the numerical lifting line method is used to describe the aerodynamic model. While assumed mode method is used to represent the structure plate model. The resulting FSI is then used for estimation of flutter speed and flutter frequency from the behavior of the generalized displacement of the plate in time and frequency domains.

In order to analysis the responses in frequency domains, Fast Fourier Transformation (FFT) technique is used to convert the generalized coordinates responses from time domain to frequency domain. At flutter condition, all the

generalized coordinates will vibrate at, nearly the same frequency, which is a flutter frequency.

The Aerodynamic Model

An unsteady panel–discrete vortex method using MATLAB computer program is devised to estimate the unsteady aerodynamic forces acting on vibrating cantilever plate, figure (1).

In this approach the plate section surface is divided into a number of panels. Each panel has vorticity strength ($\gamma_i(s)$) which change linearly along panel as given in the following equation:

$$\gamma(s_j) = \gamma_j + \frac{s_j}{L_j}(\gamma_{j+1} - \gamma_j) \quad \ldots(1)$$

The plate has unsteady motion (eg. heaving motion), wake vortices will be created behind the plate therefore; the velocity components at each mid point of panel are [6]

$$u_{pi} = V_\infty \cos\alpha + \sum_{j=1}^{N} u_{vij} + \sum_{k=1}^{NV} u_{vik} + V_{FRiy}$$

$$v_{pi} = V_\infty \sin\alpha + \sum_{j=1}^{N} v_{vij} + \sum_{k=1}^{NV} v_{vik} + V_{FRiz} \quad \ldots(2)$$

In heaving motion the induced velocity $V_{FRiy} = 0$ and V_{FRiy} may be approximated by [6]

$$V_{FRiz} = \frac{\delta_{im} - \delta_{im-1}}{\Delta t} \quad \ldots(3)$$

Where

δ_i is the displacement of each mid point of panel at each time step comes from vibrated plate .

By using the flow tangency condition (4) , Kutta condition Eq.(5) and condition of constant circulation around airfoil Eq (6)

$$\vec{V}.\vec{n} = 0 \quad \ldots(4)$$

$$\gamma_1 = \gamma_{N+1} = 0 \quad \ldots(5)$$

$$\Gamma_m + \sum_{k=1}^{NV} \Gamma_{vk} = 0 \quad \ldots(6)$$

where

$$\Gamma_m = \sum_{J=1}^{N} L_j[(\gamma_j)_m + (\gamma_{j+1})_m] \quad \ldots(7)$$

This leads to the set of linear algebraic equations with unknowns γ_j and Γ_k .These equations are solved by using Gauss elimination with partial pivoting technique to find γ_i and Γ_k [7]. Then the unsteady pressure coefficient at each time step can be obtained from

$$Cp_i = 1 - \frac{\gamma_i^2}{V_\infty^2} - \frac{2}{V_\infty^2}\left(\frac{\phi_m - \phi_{m-1}}{\Delta t}\right)_i \quad \ldots(8)$$

Equation (8) was derived from the unsteady Bernoulli's equation. The unsteady aerodynamic coefficients at different sections along the semi span at time t_m are determined by integrating the pressure distribution.

To extend the 2-D aerodynamics solution to 3-D, the effective angle of attack at each section along the span must be taken into consideration. The numerical solution for the lifting line theory developed by Anderson, et al [8] is used to determine the angle at each section. Then the unsteady effective angle may be calculated from Eq (9) [7]

$$\alpha_{eff} = \text{angle of attack at each section} + \tan^{-1}\frac{\text{heaving velocity}}{\text{flow velocity}} \quad \ldots(9)$$

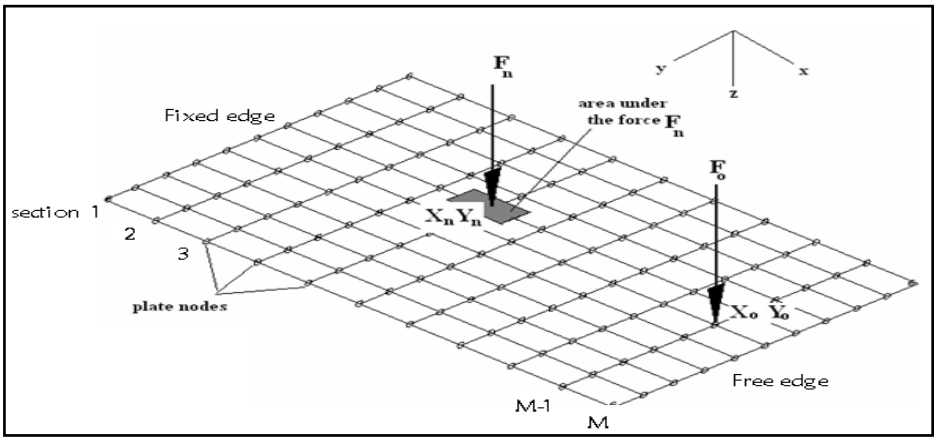

Figure (1) Three dimensional plate

Structural Model of a Three Dimensional Plate

The assumed –mode method is used in the derivation of the equations of motion for the plate. This method depends on assuming suitable solution to the displacements of the problem. In plate problem the displacements are assumed to be of the form

$$w(x,y,t) = \psi_1(x,y)q_1(t) + \psi_2(x,y)q_2(t) + \psi_3(x,y)q_3(t) + \ldots\ldots\psi_i(x,y)q_i(t) \quad \ldots(10)$$

Where

$q_i(t)$ generalized coordinates, and $\psi_i(x,y) = X_m(x)Y_n(y)$ are the admissible beam functions. $X_m(x)$ satisfy clamped-free boundary conditions and $Y_n(y)$ free-free conditions, which are defined as follows [9]:

$$X_m(x) = \mu_m(\cosh\alpha_m\frac{x}{a} - \cos\alpha_m\frac{x}{a}) - \upsilon_m(\sinh\alpha_m\frac{x}{a} - \sin\alpha_m\frac{x}{a})$$

$$\mu_m = \frac{\cosh\alpha_m + \cos\alpha_m}{\sinh\alpha_m \sin\alpha_m}, \qquad \upsilon_m = \frac{\sinh\alpha_m - \sin\alpha_m}{\sinh\alpha_m \sin\alpha_m} \qquad \ldots (11)$$

where

$\alpha_1 = 1.875, \alpha_2 = 4.694, \alpha_3 = 7.854, \ldots$ $Y_1(y) = 1$, $Y_2(y) = \sqrt{3}(2\frac{y}{b} - 1)$

$$Y_n(y) = \kappa_n(\cosh\beta_n\frac{y}{b} + \cos\beta_n\frac{y}{b}) - \lambda_n(\sinh\beta_n\frac{y}{b} + \sin\beta_n\frac{y}{b})$$

$$\kappa_n = \frac{\cosh\beta_n - \cos\beta_n}{\sinh\beta_n \sin\beta_n}, \qquad \lambda_n = \frac{\sinh\beta_n + \sin\beta_n}{\sinh\beta_n \sin\beta_n} \qquad \ldots(12)$$

where

β_n are the roots of $\cosh\beta_n \cos\beta_n = 1$

The strain energy of plate is

$$U = \frac{1}{2}\frac{Eh^3}{1-\upsilon^2}\iint_A (\nabla^2 w)^2 + 2(1-\upsilon)[(w_{xy})^2 - w_{xx}w_{yy}]\ dA \qquad \ldots(13)$$

The plate kinetic energy is

$$T = \frac{1}{2}\iint_A m\dot{w}^2\, dxdy \qquad \ldots(14)$$

Substituting Eq. (10) into Eqs (13&14) and applying Lagrange's equation the differential equations of plate motion are obtained

$$[m]\{\ddot{q}\} + [k]\{q\} = \{Q\} \qquad \ldots(15)$$

Where

$$m_{ij} = \int_A m\psi_i\psi_j\, dA, \qquad k_{ij} = \sum_{q=1}^{2}\sum_{p=1}^{2} a_{ijpq} + 2(1-\upsilon)(b_{ij} - a_{ij12})$$

$$a_{ijpr} = \frac{Eh^3}{12(1-\upsilon^2)}\iint_A \frac{\partial^2\psi_i}{\partial x_p^2}\frac{\partial^2\psi_j}{\partial x_r^2}dA \ , b_{ij} = \frac{Eh^3}{12(1-\upsilon^2)}\iint_A \frac{\partial^2\psi_i}{\partial x_1\partial x_2}\frac{\partial^2\psi_j}{\partial x_1\partial x_2}dA \qquad p = 1,2 \ \& \ r = 1,2$$

In present analysis, $x_1 = x$ and $x_2 = y$

Fully Coupled Fluid-Structure Interaction Procedure

The essential feature of the present aeroleastic model is the innovative way of interaction between the structure model and aerodynamic model.

The plate is divided into N panels and M sections in semispan. Therefore, there are N×M nodes. Each node on the plate exactly faces the nodes on upper and lower surfaces of the plate section in aerodynamic model. During vibration, the upper and lower nodes (A and B) on the plate section take their displacements from corresponding node P on the plate as shown in figure (2).

The solution starts by assuming that the plate is disturbed by initial displacements. Equation (15) is solved by using Runge-Kutta method to obtain generalized displacements. Implementation of Eq (10) the displacement of the plate at each node and at each section is determined. These displacements are fed to the aerodynamic model. Solving this model gives pressure difference (Δp) at each node and at each time step (one iteration). Finally these pressure differences are fed to the structural model (cantilever plate) Eq (15) as a part of the generalized forces Q_i.Eq.(17)

$$Q_i = \iint_A \Delta p(x, y, t)\psi_i(x, y)dxdy \qquad \ldots(17)$$

During the development of the present model the pressure differences in equation (17) were found as a mathematical function of the independent variables *x & y* of nodes plate at each time step. This can be achieved by using curve fitting between pressure differences and *x,y* coordinates of nodes at each time step . However, it was found that more accurate and economic solution may be obtained by converting the pressure (ΔP_n) to concentrated force (F_n) by multiplying the value of pressure at each node by adjacent area of the node (A_n). Then these forces (F_n) will be introduced into Eq.(17) as shown below:

$$Q_i = -\sum_{n=1}^{NS} F_n\psi(x_n, y_n) + F_o \sin(wt)\psi(x_o, y_o) \qquad \ldots(18)$$

Where

x_n and y_n are the position of the nodes on the cantilever plate; x_o and y_o are the position of excitation force (if exist) on the plate as shown in figure (1). F_n can be written as [10]

$$F_n = A_n \Delta p_n \qquad \ldots(19)$$

Numerical solution in the present work have shown that the time interval is a very important parameter to obtain physically realistic results.

It was observed that numerical instability can occur depending on the chosen time interval for certain air speed and certain plate .

One should be very careful when analyzing the results, to avoid a numerical instability to be interpreted as a physical instability (flutter). This problem has been resolved by taking an initial value for the time interval. This value was then decreased until no noticeable difference between consecutive solutions was observed.

For calculations, the number of spanwise sections and surface panels employed for different plates were 10 sections and 60 surface panels. The plate cross section configuration is shown in figure (2) where the rounded ends prevent any discontinuity during penalization process[10].

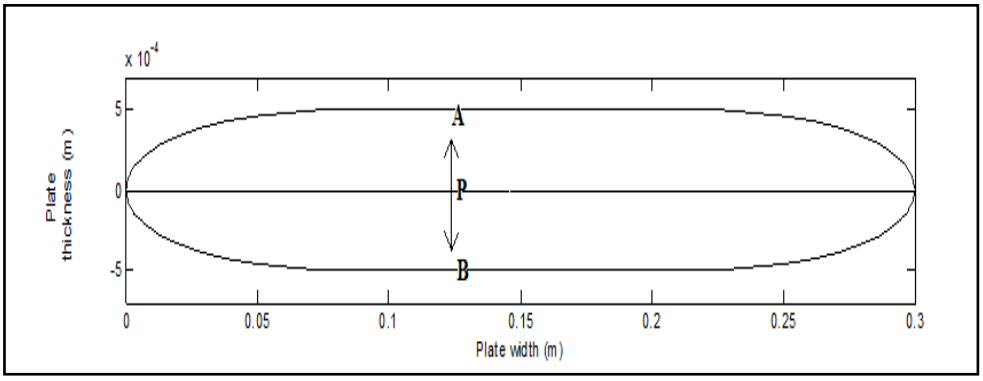

Figure (2). Modified plate section configuration

Experimental work

The validity of the present structure and aerodynamic theoretical models will be tested through comparisons with measurements. For this purpose, plates flutter experiments have been carried out in a wind tunnel.

The experiments were conducted in an open circuit type, low speed wind tunnel (manufactured by Plint & Partners LTD.) of 315 mm×315 mm cross section and test section length of 610mm. The air mean velocity at the test section was 35 m/sec.

Figure (3) Nine test samples of cantilever plates

The Vibration Measurements includes: a piezoelectric accelerometer (B&K 4370) is attached to the plate to measure the vibration. The signal which comes from the accelerometer is passed through a conditioning amplifier (B&K2626). This signal was then fed into a built-in FFT oscilloscope type (ATTEN-ADS 1022c 25MHZ) and to the PC interface (Easyscope 3.0computer software system).
Nine aluminum cantilever plates of 0.7mm thickness were tested as shown in figure (3). The aim of these experiments is to determine the flutter speeds and flutter frequencies for the plates.

The test rig assembly is shown in figure (4) and the following steps were followed:-

1-The selected plate was mounted in the test section vertically. The root of the plate was fixed by the external rigid frame .Care was taken to minimize clearance between plate tip and floor of the test section.
2- The accelerometer was fixed on the plate at a distance 35 mm from the root.
3- The Pitot static tube was mounted in the upstream end of the test section.
4- The connections were made as shown in figure (4-b)
5- The test section was closed. The air speed control valve was adjusted to the low speed position, and the fan was then operated.
6- The air speed was increased gradually by means of control valve. In the mean time the behavior of the plate oscillation was observed.
7- At the threshold of divergent oscillation the air speed was measured. This speed may be considered as the flutter speed of the plate when the destabilization action becomes greater than the stabilizing forces and the oscillations diverge.
8- The time history of the plate response was recorded by the oscilloscope.
9- Steps (1-8) were repeated for all other plates.
The experiments were performed in Machines and Equipment Department-University of Technology / Baghdad –Iraq.

Results and discussion

The validity of the present method will be tested through comparisons with the related published works and with wind tunnel measurements.

Comparison with Related Published Models

Nejad and Skokrollahi [2] calculated the flutter speed and flutter frequency for cantilever plates using eigen mode flutter analysis. Three plates (their specifications are given in table (1)) were selected for comparison purpose. The aeroelasticity responses of these plates were resolved by using the present FSI model. The results are shown in figures (5) for plate No.1 at V=40.1 as example of the time responses of the first four generalized displacements and their FFT analysis .A few modes are necessary to obtain a solution with good precision [11].

In figures (5a), the generalized displacements in all modes show a periodic motion . Therefore, the onset of flutter condition is reached and the air speed at this moment may be considered as the flutter speed. The general trend of the curves seems to be in a good agreement with similar simulations [12].
The flutter frequency of plate No.1 may be estimated from figures (5b), when all the modes are vibrating at identical frequencies. The final results are shown in table (2) for three plates. Both flutter speed and corresponding flutter frequency are increased

as the aspect ratio decreases. The comparison in table (2) confirms the validity of the present method; however, the present calculated values are slightly underpredicted in comparison with Ref [2]. The reasons may be attributed to the difference in technique of estimating the flutter speed and flutter frequency, as has already been mentioned. Also, the exact values of material properties of the plates and the plate cross section configuration were not supplied by Nejad and Skokrollahi [2], therefore, assumed values of modulus of elasticity and density of Aluminum where used (table (1)).

Table (1) Specification of the selected plate [2]

Plate No.	Dimension (m)	Aspect ratio	Modulus of elasticity (N/m^2)	Density (kg/m^3)	Poisson's ratio
1	0.001*0.3*0.3	1	70×10^9	2700	0.3
2	0.001*0.3*0.6	2			
3	0.001*0.3*1.5	5			

Table (2) Comparison between present work and reference [2]

Plate No.	V_f (m/sec) present work	V_f (m/sec) Ref [2]	Flutter frequency (rad/sec) present work	Flutter frequency (rad/sec) Ref [2]
1	40.1	42	73.6	76
2	13.7	15	33.4	35
3	4.3	5	10.3	11

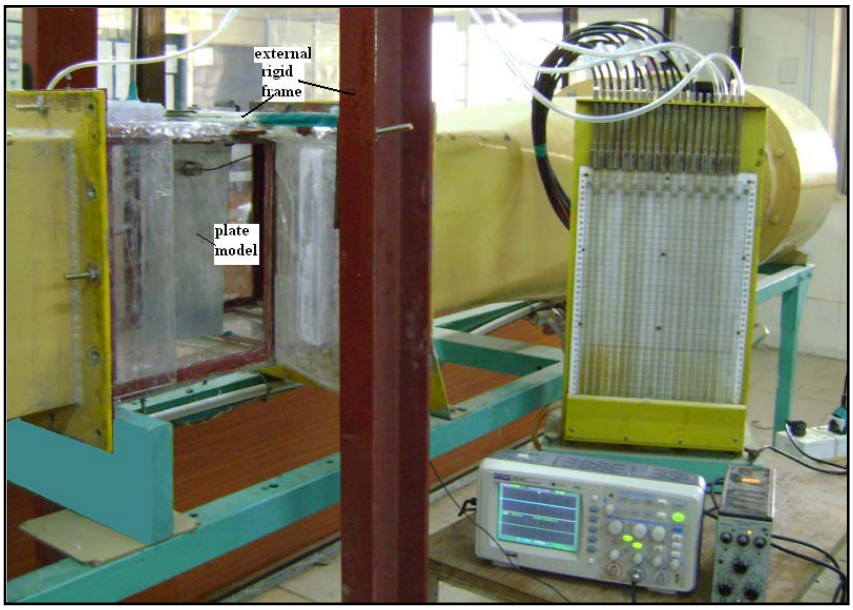

a- Photograph

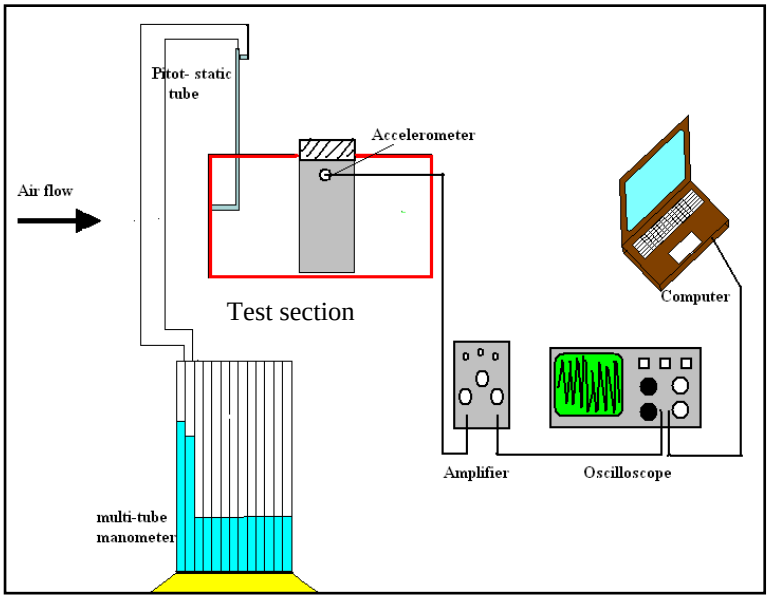

b- layout

Figure (4) General view of plates flutter experiment

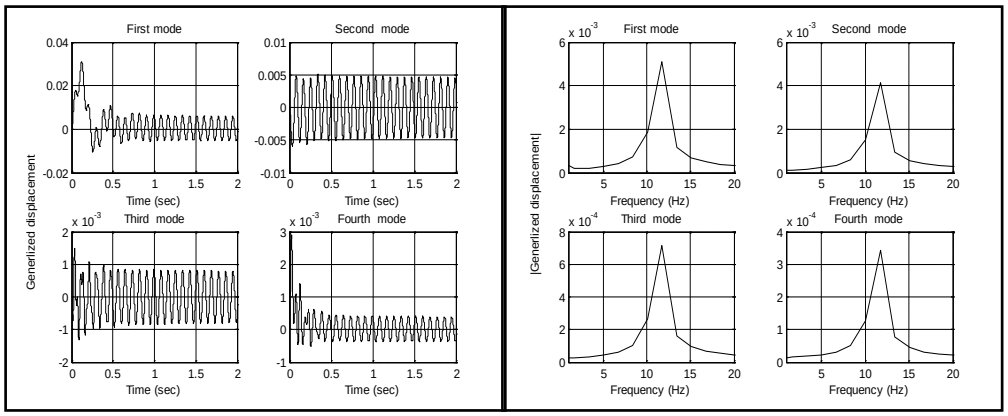

(a) Time responses (b) FFT analysis

Figure (5) Responses of the generalized displacements and their FFT for plate No.1

Comparison with Wind Tunnel Measurements

The set of experiments was concerned with the measurement of flutter speed and flutter frequency at flutter condition for three groups of cantilever plates. Each group consists of three plates of equal width (chord) but of different length (span). Results of representative plates from each group will be shown.

Figures (6 to 9) show the theoretical time responses of the generalized displacements and their FFT analysis for plate B (group No.1). When the air speed is below the flutter speed, the aerodynamic damping is strongly evidenced for all modes, as shown in figure (6a) and (7a), and the responses reach finally to the plat static equilibrium position. The plate is vibrating at different damping frequencies for each mode, as shown in figures (6b) and (7b). In figure (8), the flutter condition is reached at V=24.7 (m/sec) since the generalized displacements in all modes show a periodic motion, that is a limit cycle oscillation. All the modes are vibrating at identical frequencies, that is a flutter frequency, as shown in figure (8b) .Beyond the flutter speed, the amplitudes of the generalized displacements grow rapidly, a diverging oscillation is then reached as shown in figure (9a).

The experimental time responses and their FFT analysis for plates B, E, H are shown in figures (10) to (12). All these figures represent the responses at flutter condition except A. The flutter frequency may be estimated by carefully examining the FFT curve of the test point for each plate. The frequency of the more repeated highest amplitude of the FFT curve may be considered as flutter frequency.

Figures (13) and (14) present a comparison of theoretical and experimental flutter speed and flutter frequency plotted as functions of aspect ratio. Both flutter speed and flutter frequency are increased as aspect ratio decreases. This increasing becomes rapid at low aspect ratio. Also, the increase in the plate chord at the same aspect ratio will reduce the flutter speed and flutter frequency. Acceptable agreement between the two results is obtained. The theoretical values are under predicted in

comparison with experiments. The flutter speed and flutter frequency are within average absolute error of about 13% and 16 % respectively.

It should be noted that, the results from the method of Dayang [13] indicated an error in flutter speed and flutter frequency of 13% and 33% respectively in comparison with experiments. Therefore, the present method shows good improvement over the method of Dayang [13]. The final results are shown in table (3). The comparison in this table confirms the validity of the present method.

Table (3) Theoretical and experimental flutter speed and flutter frequency for cantilever plates

Group No.	Type	Plate dimensions (cm) & Aspect ratio	V_f (m/sec) Exp.	V_f (m/sec) Th.	ω_f (Hz) Exp.	ω_f (Hz) Th.
1	A	10*21 2.1	Above 35 m/sec	32.7		19.53
	B	10*24 2.4	28.5	24.7	20.51	17.58
	C	10*28 2.8	25	22.5	18.55	16.63
2	D	15*17 1.13	Above 35 m/sec	31.5	-	16.8
	E	15*22 1.46	28	26.1	16.6	13.67
	F	15*28 1.86	23	20.4	13.67	11.72
3	G	20*20 1	31	27	16.6	14.09
	H	20*25 1.25	24.8	21.7	14.65	12.08
	I	20*28 1.4	22.2	19.3	12.7	10.07

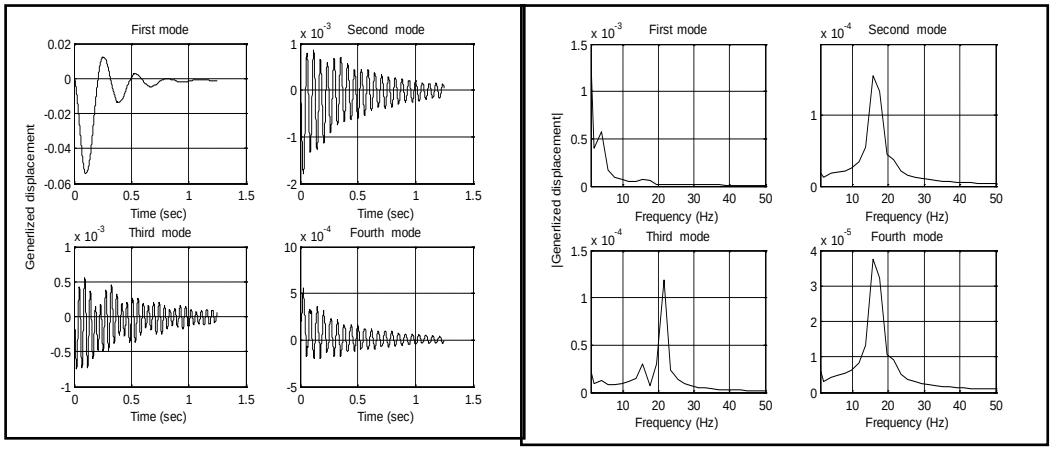

(a) Time responses (b) FFT analysis

Figure (6) Theoretical responses of the generalized displacements and their FFT analysis for plate type-B at V=15 (m/sec) (below flutter speed)

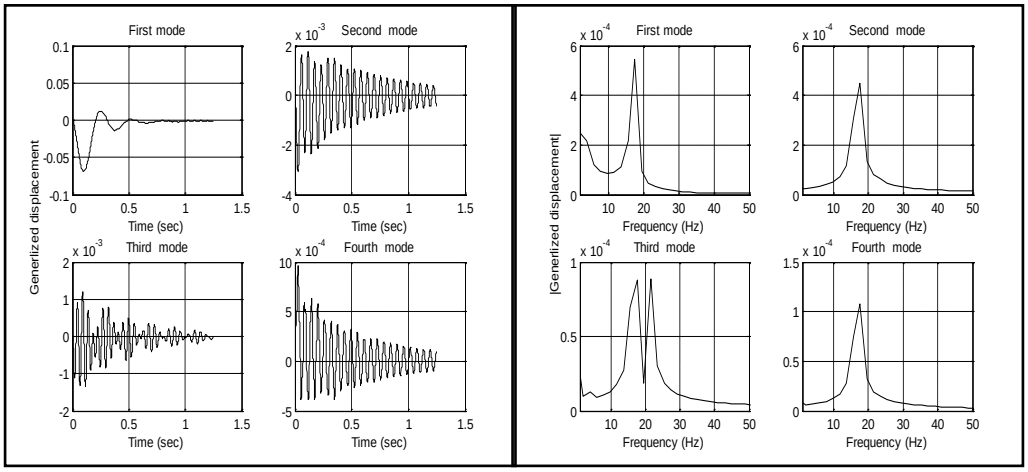

(a) Time responses (b) FFT analysis

Figure (7) Theoretical responses of the generalized displacements and their FFT analysis for plate-B at V=20 (m/sec) (below flutter speed)

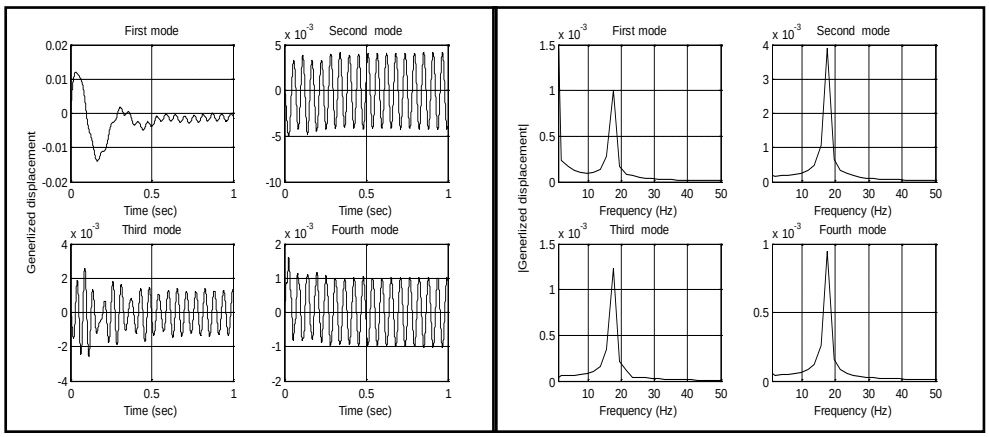

(a) Time responses (b) FFT analysis

Figure (8) Theoretical responses of the generalized displacements and their FFT analysis for plate-B at V=24.7 (m/sec) (flutter condition)

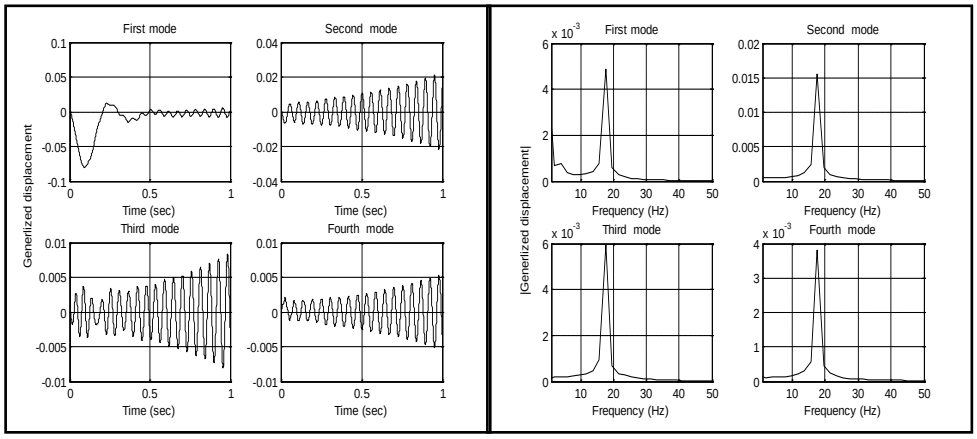

(a) Time responses (b) FFT analysis

Figure (9) Theoretical responses of the generalized displacements and their FFT analysis for plate-B at V=26 (m/sec)(beyond flutter speed)

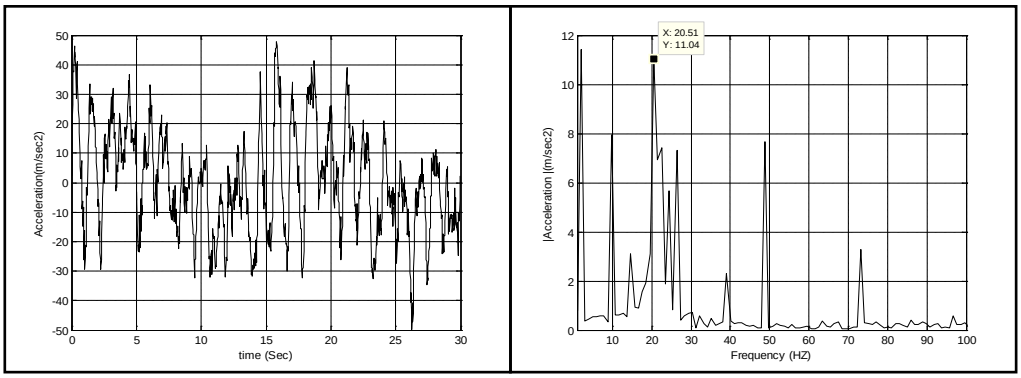

(a) Time responses (b) FFT analysis

Figure (10) Experimental responses of the test point and their FFT analysis for plate -B at corrected flutter condition (V=28.9 (m/sec))

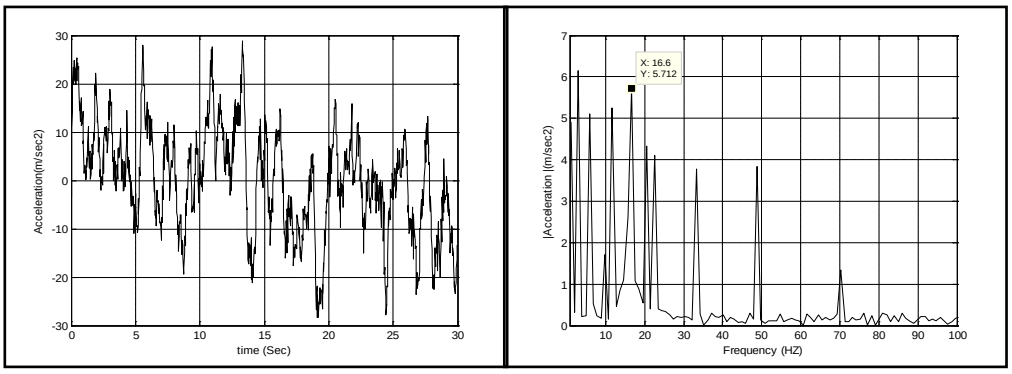

(a) Time responses (b) FFT analysis

Figure (11) Experimental responses of the test point and their FFT analysis for plate -E at corrected flutter condition (V=28.4 (m/sec))

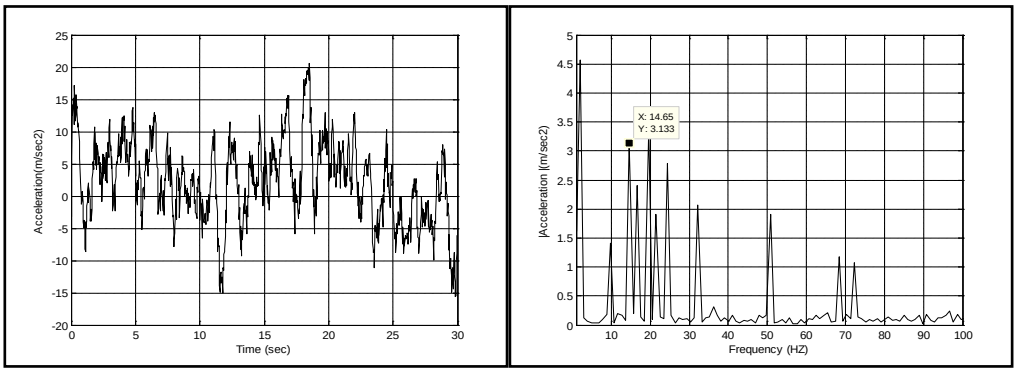

(a) Time responses (b) FFT analysis

Figure (12) Experimental responses of the test point and their FFT analysis for plate -H at corrected flutter condition (V=25.2 (m/sec))

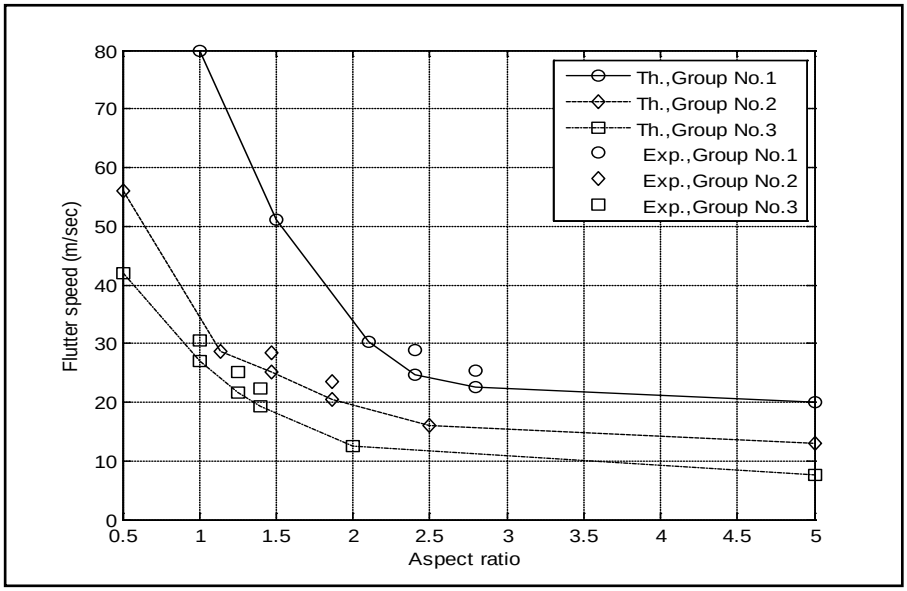

Figure (13) Effect of plate aspect ratio on flutter speed

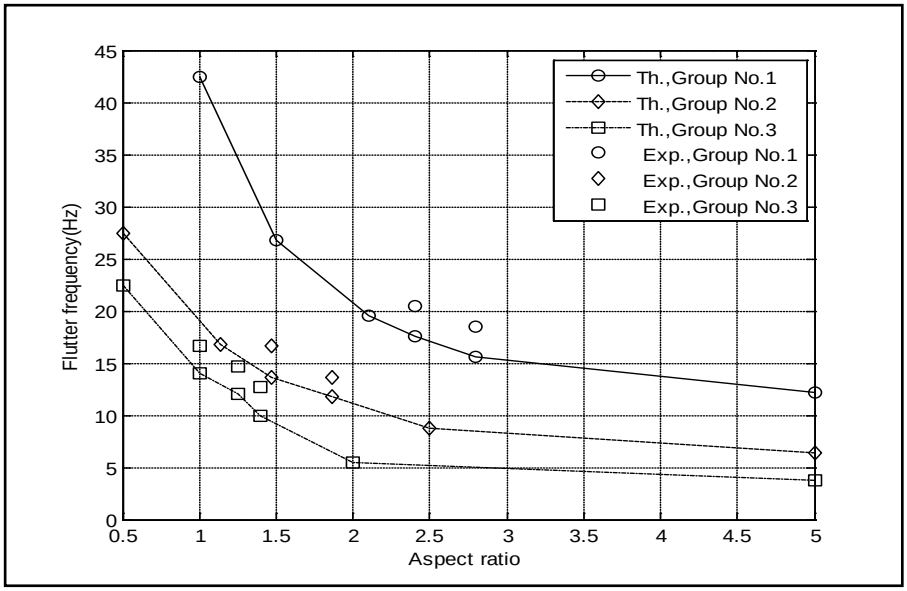

Figure (14) Effect of plate aspect ratio on flutter frequency

CONCLUSIONS

According to the obtained results, the following can be concluded:

1- The difficult task in FSI solution is the way of exchanging the aerodynamic forcing and structural displacement within each iteration. The fitting surface curve may be used to obtain the pressure distribution as function of coordinates system. However, fitting in three dimensions is inaccurate and needs a huge amount of computer memory and processing time during execution. In the present work, this difficulty was solved by converting the pressures to concentrated forces by multiplying the

value of pressure at each node by adjacent area of the node. Then these forces will be introduced to the structure equation as discrete forces.
2- In FSI system, the natural frequencies of the system become function of the properties of the structure plus the external variables like speed of media that is surrounding the structure.
3-The aerodynamic effect at speeds below the flutter speed may contribute damping the external vibration until at resonance cases.
4- Both flutter speed and flutter frequency are increased as aspect ratio decreases and this increasing becomes rapid at low aspect ratio less than 2.
5- The increase in the plate chord at the same aspect ratio will reduce the flutter speed and flutter frequency.

REFERENCES

[1] Hodges D. H. "Introduction to Structural Dynamics and Aeroelasticity" Cambridge University press, 2002.
[2] Nejad F.B and Shokrollahi S ,"Three-Dimensional Eigenmode Flutter Analysis of a Rectangular Cantilever Plate in Low Subsonic Flow", Scientia Iranica, Vol 11, pp60-68, 2004.
[3] Eloy C. and Souilliez C. "Flutter of a Rectangular Plate", Journal of Fluids and Structures, Vol. 23, pp. 904-919, 2007.
[4] Chen X-Y, Zha G-C, and Hu Z-J. "Numerical Simulation of Flow Induced Vibration Based on Fully Coupled-Structural Interactions", AIAA pp 2004-2240, June 28–July 1; 2004.
[5] Chen X, and Zha G-C " Fully Coupled Fluid-Structural Iinteractions Using an Efficient High Solution Upwind Scheme" Journal of Fluid and Structure, Vol. 20, pp. 1105–1125, 2005.
[6] Abu-Tabikh,M.I." Modeling of Steady and Unsteady Turbulent Boundary Layer Separation Using Vortex Hybrid Method ", Ph.D thesis, Department of Mechanical Engineering, U.O.T, Baghdad, 1997.
[7] Mantia , M. L.and Dabnichki,P." Unsteady Panel Method for Flapping Foil", Engineering Analysis with Boundary Elements, Vol.33, pp.572-580, 2009.
[8] Anderson, Jr., J.D. , Corda,S. and Van Wie , D.M. "Numerical Lifting Line Ttheory Applied to Drooped Leading –Edge Wing Below and Above Stall",Journal of Aircraft ,Vol. 17 ,No.12, pp.898-904, 1980.
[9] Chiba, M. and Sugimoto,T. "Vibration Characteristics f a Cantilever Plate With Attached Spring-Mass System", Journal of Sound and Vibration,Vol. 260,pp. 237-263, 2003.
[10] Al-Araji H. "Vibration Assessment of Aerodynamic Loads on Low Speed Aircraft Wings " Ph.D thesis, Department of Mechanical Engineering, U.O.T, Baghdad, 2012.
[11] Abbas L K, Chen1 Q. and Milanese A. " Non-Linear Aeroelastic Investigations of Store(s)-Induced Limit Cycle Oscillations", J. Aerospace Engineering Vol. 222 Part G, 2008.
[12] Benini, G.R., Belo, E.M. and Marques, F.D. "Numerical Model For Simulation of Fixed Wings Aeroelastic Response",J.of the Braz. Soc. of mech. Sci. Eng., Vol. XXVl, No.2/129,pp129-136, 2004.
[13] L.A. Dayang " LCO Flutter of Cantilevered Woven Glass/Epoxy Laminate in Subsonic Flow" ,Acta Mechanica Sinica,Vol.24mNo.1pp.107-110,2008.